Paper ID APEN-MIT-2019_139
Applied Energy Symposium: MIT A+B
May 22-24, 2019 • Boston, USA

The Modelling and Optimization of Distributed Network Based on Source-Limit Infrastructure

Songshan Guo
Power and Control Systems Research Laboratory
University of Warwick
Coventry, England,UK
s.guo.5@warwick.ac.uk

Jihong Wang
Power and Control Systems Research Laboratory
University of Warwick
Coventry, England,UK
Jihong.wang@warwick.ac.uk

***Abstract*—**In this paper, a hybrid optimization algorithm combined Multi-Objective Dragonfly Algorithm (MODA) with time-varying management is presented to search optimal power flow of distributed power network. A numerical model is built to simulate and investigate the impact of intermittent energy and the change of load demand. Then, the distributed battery generators are integrated into the distribution network to compensate the above negative impact. The objectives consist of minimizing power losses, improving the voltage stability by searching the optimal placement of distributed battery systems. The algorithm is proven to be effective and it also has the potential to be used in the planning of any Smart Grid (SG) system.

Keywords—*System modelling, Optimal placement, Battery storage, MODA*

I. INTRODUCTION

The electrical energy system is currently undergoing a paradigm change, that has been affected by a change from the traditional centralized grid to a more decentralized system. Many factors contribute to this change: government policies, steady urbanization, environmental consideration. As a result, the future grid will be the way that generation and demand is kept in balance, which means the power flow is bi-directional. In this case, most of the infrastructure of distribution need to be updated to keep the network safe, especially for the residential distribution network. However, this will increase the network cost and it does not worth investing. Furthermore, some areas are hard to upgrade the infrastructure due to the limit of area and capacity.

For this problem, many attempts have been made in recent years to solve it by applying different methodologies. The microgrid management system is proposed by many researchers, such as the hybrid energy systems [1]. An analytical method was firstly introduced in 2004[2] to searching the optimal placement of a single (Distributed Generators) DGs in both radial and meshed networks to minimize power losses of the transmission system. However, this approach only optimizes siting and considers DGs sizing as fixed. Some simulations-based validation in a microgrid are also studied to verify the management and control system [3-4]. The management of conventional generation and enabling energy among neighboring microgrids have been proposed in [5-6]. The V2G technologies are used to take part in the peak shifting in [7]. The energy storage plays an increasingly important role in microgrid balancing for the purpose of integrating the intermittent renewable energy [8-9], since it can keep the energy within the network limit by charging/discharging energy. The upgrade of the distributed network will also improve this situation, but it is not a cost-effective way. How to rationally plan new energy resources in the source-limit distribution network is an urgent problem to be solved.

The rest of paper is organized as follows. Section 2 presents the modelling of source limited distribution network based on European low voltage test feeder. Section 3 analyzes the impact on conventional distribution network with random installed renewable energy generation. Section 4 shows the optimized placement of the battery in terms of optimal power flow. Section 5 concludes the paper and the future work plan.

II. MODELLING OF DISTRIBUTION NETWORK

GridLAB-D [10] is a new power distribution system simulation and analysis tool that can produce valuable information in power distribution system design and operation, especially, help the utilities that wish to take advantage of the latest energy technologies. It incorporates the most advanced modeling techniques with high-performance algorithms to deliver the robust results in end-use modeling. It is capable of studying distribution network utility behavior range from a few to few tens' seconds, simulating the interaction between physical phenomena, business models, markets and regional economics, and consumer behaviors. It creates a flexible simulation environment that can be integrated with a variety of third-party data management and analysis tools, such as MATLAB. Concerns expressed by utility engineers, regulators, various stakeholders, and consumers can be addressed by GridLAB-D.

For the power-flow solver, both current and power mismatch method are proposed. The complex current and power mismatch at a given bus *k* are given by [11]

$$\Delta I_k = \frac{P_k^{sp} - jQ_k^{sp}}{E_k} - \sum_{i=1}^{n} Y_{ki} E_i = 0 \quad (1)$$

$$\Delta P_k = P_k^{sp} - \sum_{i=1}^{n} |V_k||V_i|(G_{ki}\cos\delta_{ki} + B_{ki}\sin\delta_{ki}) \quad (2)$$

where E_k is the complex conjugated voltage phase at bus *k*. P_k^{sp} and Q_k^{sp} are specified active and reactive power at bus *k*. B_{ki} is the susceptance of the n^{th} bus admittance, G_{ki} is the conductance of the n^{th} bus admittance. V_i is the voltage at bus *i*.

The P_k^{sp} and Q_k^{sp} can be calculated by using the difference between power from generator and power from load.

$$P_k^{sp}=P_{G(k)}-P_{L(k)} \tag{3}$$

$$Q_k^{sp}=Q_{G(k)}-Q_{L(k)} \tag{4}$$

where, $P_{L(k)}$ and $Q_{L(k)}$ can be modeled in polynomial form:

$$P_{L(k)}=P_{0k}(a_p+b_pV_k+c_pV_k^2) \tag{5}$$

$$Q_{L(k)}=Q_{0k}(a_q+b_qV_k+c_qV_k^2) \tag{6}$$

where:

$$a_p+b_p+c_p=1 \tag{7}$$

$$a_q+b_q+c_q=1 \tag{8}$$

In Equation (1)-(2), the Jacobian matrix is used to represent the power and current mismatches load flow method through NR method.

$$\begin{bmatrix} \Delta I_{m1} \\ \Delta I_{r1} \\ \vdots \\ \Delta P_k \\ \vdots \\ \Delta I_{mn} \\ \Delta I_{rn} \end{bmatrix} = \begin{bmatrix} \frac{\partial I_{m1}}{\partial V_{r1}} & \frac{\partial I_{m1}}{\partial V_{m1}} & \cdots & \frac{\partial I_{m1}}{\partial \delta_k} & \cdots & \frac{\partial I_{m1}}{\partial V_{rn}} & \frac{\partial I_{m1}}{\partial V_{mn}} \\ \frac{\partial I_{r1}}{\partial V_{r1}} & \frac{\partial I_{r1}}{\partial V_{m1}} & \cdots & \frac{\partial I_{r1}}{\partial \delta_k} & \cdots & \frac{\partial I_{r1}}{\partial V_{rn}} & \frac{\partial I_{r1}}{\partial V_{mn}} \\ \vdots & \vdots & \vdots & \vdots & \vdots & \vdots & \vdots \\ \frac{\partial P_k}{\partial V_{r1}} & \frac{\partial P_k}{\partial V_{m1}} & \cdots & \frac{\partial P_k}{\partial \delta_k} & \cdots & \frac{\partial P_k}{\partial V_{rn}} & \frac{\partial P_k}{\partial V_{mn}} \\ \vdots & \vdots & \vdots & \vdots & \vdots & \vdots & \vdots \\ \frac{\partial I_{mn}}{\partial V_{r1}} & \frac{\partial I_{mn}}{\partial V_{m1}} & \cdots & \frac{\partial I_{mn}}{\partial \delta_k} & \cdots & \frac{\partial I_{mn}}{\partial V_{rn}} & \frac{\partial I_{mn}}{\partial V_{mn}} \\ \frac{\partial I_{rn}}{\partial V_{r1}} & \frac{\partial I_{rn}}{\partial V_{m1}} & \cdots & \frac{\partial I_{rn}}{\partial \delta_k} & \cdots & \frac{\partial I_{rn}}{\partial V_{rn}} & \frac{\partial I_{rn}}{\partial V_{mn}} \end{bmatrix} \begin{bmatrix} \Delta V_{r1} \\ \Delta I_{m1} \\ \vdots \\ \Delta \delta_k \\ \vdots \\ \Delta V_{rn} \\ \Delta V_{mn} \end{bmatrix} \tag{9}$$

where ΔI is current mismatch to the bus, k is bus number, P is active power component of a load, Q is reactive power component of a load, V_{ri} represents the real part of the voltage, V_{mi} represents the imaginary part of the voltage, δ_k represents the phase angle.

At the bus *k* of PQ bus, the derivation of diagonal elements can be written as

$$\frac{\partial I_{mk}}{\partial V_{rk}}=B_{kk}-a_k \tag{10}$$

$$\frac{\partial I_{mk}}{\partial V_{mk}}=G_{kk}-b_k \tag{11}$$

$$\frac{\partial I_{rk}}{\partial V_{rk}}=G_{kk}-c_k \tag{12}$$

$$\frac{\partial I_{rk}}{\partial V_{mk}}=-B_{kk}-d_k \tag{13}$$

where a_k , b_k , c_k d_k can be shown in (14)-(17)

$$a_k=\left[\frac{Q_k^{'}(V_{rk}^2-V_{mk}^2)-2P_k^{'}V_{rk}V_{mk}}{V_k^4}+\frac{V_{rk}b_pP_{0k}V_{mk}+b_pQ_{0k}V_{mk}^2}{V_k^3}+c_qQ_{0k}\right] \tag{14}$$

$$b_k=\left[\frac{P_k^{'}(V_{rk}^2-V_{mk}^2)+2Q_k^{'}V_{rk}V_{mk}}{V_k^4}-\frac{b_pQ_{0k}V_{mk}V_{rk}+b_pP_{0k}V_{rk}^2}{V_k^3}-c_pP_{0k}\right] \tag{15}$$

$$c_k=\left[\frac{P_k^{'}(V_{rk}^2-V_{mk}^2)-2Q_k^{'}V_{rk}V_{mk}}{V_k^4}+\frac{b_pQ_{0k}V_{mk}V_{rk}-b_pP_{0k}V_{mk}^2}{V_k^3}-c_pP_{0k}\right] \tag{16}$$

$$d_k=\left[\frac{Q_k^{'}(V_{rk}^2-V_{mk}^2)-2P_k^{'}V_{rl}V_{ml}}{V_k^4}+\frac{V_{ml}b_pP_{0k}V_{mk}-b_qQ_{0k}V_{rk}^2}{V_k^3}-c_qQ_{0k}\right] \tag{17}$$

where:

$$P_k^{'}=P_{G(k)}-P_{0k}a_p \tag{18}$$

$$Q_k^{'}=Q_{G(k)}-Q_{0k}a_q \tag{19}$$

The off diagonal elements are formulated as

$$\frac{\partial I_{mk}}{\partial V_{ri}}=B_{ki} \tag{20}$$

$$\frac{\partial I_{mk}}{\partial V_{mi}}=G_{ki} \tag{21}$$

$$\frac{\partial I_{rk}}{\partial V_{ri}}=G_{ki} \tag{22}$$

$$\frac{\partial I_{rk}}{\partial V_{mi}}=-B_{ki} \tag{23}$$

For the PV buses, the derivation of diagonal elements at bus *k* can be written as

$$\frac{\partial P_k}{\partial \delta_k}=-V_k\sum_{\substack{i=1\\ i\neq k}}^{n}(G_{ki}\sin\delta_{ki}-B_{ki}\cos\delta_{ki}) \tag{24}$$

The off diagonal elements are formulated as

$$\frac{\partial I_{mk}}{\partial \delta_k}=V_k(G_{kk}\cos\delta_k-B_{kk}\sin\delta_k) \tag{25}$$

$$\frac{\partial I_{rk}}{\partial \delta_k}=-V_k(G_{kk}\cos\delta_k+B_{kk}\sin\delta_k) \tag{26}$$

$$\frac{\partial P_k}{\partial V_{mi}}=V_k(G_{ki}\sin\delta_k-B_{ki}\cos\delta_k) \tag{27}$$

$$\frac{\partial P_k}{\partial V_{ri}}=V_k(G_{ki}\sin\delta_k+B_{ki}\cos\delta_k) \tag{28}$$

Fig.1 represents the one-line diagram of buses *j* and *j*+1. The amount of power that can be transmitted through the lines is limited by several factors, including the material itself and the temperature of the environment. This limitation is observed as a decrease in power transmission from the source to the destination, called power loss. The power loss of the distribution network is an important criterion in evaluating a network, which can be formulated by:

$$P_{loss}=\sum_{i=1}^{N}R_i\times\frac{(P_{m2}^2+Q_{m2}^2)}{V_{m2}^2}+j\sum_{i=1}^{N}X_i\times\frac{(P_{m2}^2+Q_{m2}^2)}{V_{m2}^2} \tag{29}$$

where P_{loss} is the total network loss, P_{m2} and Q_{m2} are the active and reactive loads at bus $m2$. V_{m2} is the voltage profile of the buses $m2$. R_i and X_i are the resistance and reactance of the branch *i*.

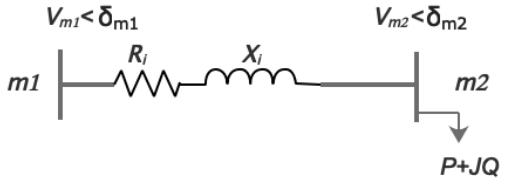

Fig. 1. One-line diadram of distribution system

The voltage stability is one of the most significant security indices under planning and operation of power system. [12] proposes a stability index for identifying the node, which is most sensitive to voltage collapse. The voltage stability index can be described as follows:

$$SI_j = |V_{j+1}|^4 - 4\left[P_j X - Q_j R_{j+1,j}\right]^2 - 4\left[P_j R_{j+1,j} + Q_j R_{j+1,j}\right]|V_j|^2 \quad (30)$$

where SI_j is voltage stability index of bus j, V_{j+1} is voltage of bus $m2$, P_j and Q_j are total buses active and reactive power feed through bus $m1$, $X_{j+1,j}$ and $R_{j+1,j}$ are the reactance and resistance between bus $j+1$ and j.

The original model for solar generation calculation is written as

$$P_{out} = I_n \cdot \eta_1 \cdot \eta_2 \cdot A \cdot T_{corr} \cdot k \quad (31)$$

where I_n is the insolation value, η_1 is the soiling factor, A is the area of solar panels, T_{corr} is the temperature correlation value and k is a constant value. T_{corr} can be illustrated as

$$T_{corr} = 1 + T_{co} \cdot (T_{cell} - 25)/100 \quad (32)$$

where T_{co} is determined by the type of solar panels.

The disadvantage of this model is that these coefficients are all changes with time, but some coefficients are fixed values and some coefficients are approximate values. For example, panel temperature is determined by wind speed, insolation and soiling factor as shown in following equations.

$$T_{\text{module}} = I_n \cdot k_1 \cdot \eta_1 \cdot e^{(\eta_{corr} + \eta_{bco} \cdot s_{wind})} + T_{amb} + I_n \cdot k_1 \cdot \eta_1 \quad (33)$$

The revised model is to generate various inputs matrix and the elements of each matrix are determined by the real monitor data, which can be illustrated as

$$M(P_{out}) = M(I_n) \cdot M(\eta_1) \cdot M(\eta_2) \cdot M(T_{corr}) \cdot M(t_{seg}) \cdot k' \quad (34)$$

To simplify the volume of elements in each matrix, the fixed time segment is selected such as 1 day. During this period, the elements of each matrix is iteratively interactive and search the optimal value for each time segment. As a result, an optimal elements table is generated for the calculation of solar generation.

The battery model is rebuilt by considering the inverter efficiency curve. From the real data, the efficiency of inverter is determined by the SOC and charging/discharging power as shown in Fig.2. The inverter efficiency is close to its upper value when the discharging/charging power gets close to 35% of rated power.

The SOC at the time t during the processes of charging, and discharging can be obtained by

$$\begin{cases} \text{Charging: } SOC_t = SOC_{t-1} + \dfrac{P_{ch}\eta_{in}\Delta t}{C_b} \\ \text{Discharging: } SOC_t = SOC_{t-1} - \dfrac{P_{dis}\Delta t}{\eta_{in} C_b} \end{cases} \quad (35)$$

where P_{dis} and P_{ch} refer to the charging and discharging power, respectively; C_b is the capacity of the battery, k_{de} is the self-decay rate, and Δt is the time interval.

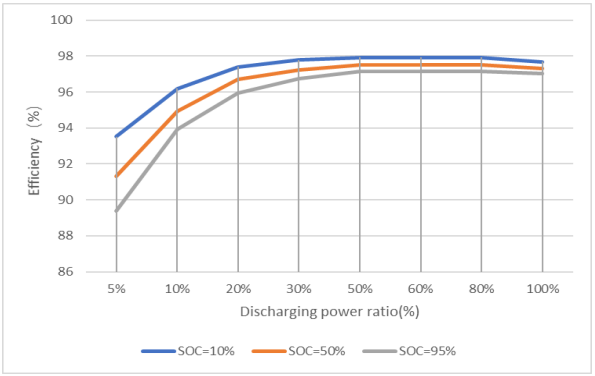

a) Discharging efficiency

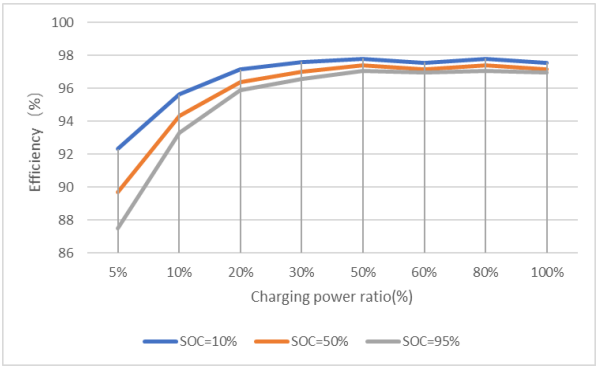

b) charging efficiency

Fig. 2. Discharging/charging efficiency of inverter

III. Optimisation Algorithms

The purpose of the MODA [13] used in this paper it to search for the optimal placement of battery installation to enhance the voltage stability and reduce the power losses. The inspiration of MODA is from the static and dynamic swarming behaviours of dragonflies. The behaviour of swarms of dragonfly follows three primitive principles: separation, alignment, cohesion. These behaviours can be mathematically described as follows:

Separation : $$S_i = -\sum_{j=1}^{N}(X - X_j) \quad (36)$$

Alignment : $$A_i = \frac{\sum_{j=1}^{N} V_j}{N} \quad (37)$$

Cohesion : $$C_i = \frac{\sum_{j=1}^{N} X_j}{N} - X \quad (38)$$

where X is the current position of the individual, X_j shows the j-th neighbouring position, V_j shows the velocity of j-th neighbouring individual, and N is the number of individuals.

The MODA is developed based on three primitive principles and the characteristics of biological populations in searching for food and avoiding natural enemies. For solving the multi-objective problem, it is firstly equipped with an archive to store and update the optimal Pareto solutions. The food source is selected from the least populated region of the obtained Pareto optimal front to increase its coverage. Secondly, there should be a management mechanism to manage the archive due to the risk of overflow because of regular updates. The principle of judgement is shown as follows:

−If at least one archive element dominates the new element, it should be forbidden to store the new element.

−If a new solution dominates some of the archive elements, the relevant archive elements should be removed and replaced by the new one.

−If the solution is not dominated by any of the archive element, it should be stored in the archive.

−One or more elements from crowded segment should be removed to store new solution if the archive is full.

The fuzzy-based decision-making algorithm is used to find the acceptable solution on the Pareto front from a set of non-dominated solutions because the output of optimisation is an optimal solution of the matrix which contains many solutions. Inputs values are mapped through set membership functions to degrees of membership in multiple sets of fuzzy variables. Each membership function is a curve ranging from 0 to 1 with the shapes normally derived from the knowledge of a human expert.

IV. Results and Analysis

The modified test feeder is developed based on the IEEE European Low Voltage Test Feeder (ELVTF)[14], shown as Fig.1. This is a low-voltage radial test grid based on a distribution system with a fundamental frequency of 50 Hz. The feeder is connected to the Medium Voltage (MV) system through a transformer at a substation. The transformer steps the voltage down from 11 kV to 416 V which is the operating voltage of the European area. The medium system is modelled as a voltage source and appropriate impedance.

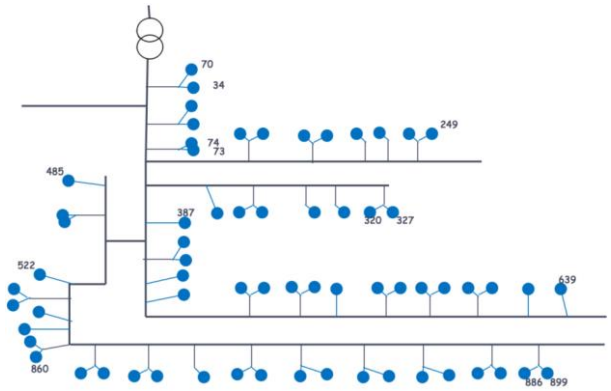

Fig. 3. European Low Voltage Test Feeder

The capacity limit of substation transformer is rated as 0.4MVA(import)/0.1MVA(export) with delta/grounded-wye connection. Line code is represented in form of impedance and admittance, shown as Table I. However, the node configuration is different from the ELVTF , because analysis of DERs will be considered in this feeder and the three-phase load is also considered.

TABLE I. Definition of Line Code in Modified Test Feeder

Name	Nphases	R1	X1	R0	X0	Units
2c_.007	3	3.97	0.099	3.97	0.099	km
2c_.0225	3	1.257	0.085	1.257	0.085	km
2c_16	3	1.15	0.088	1.2	0.088	km
35_SAC_XSC	3	0.868	0.092	0.76	0.092	km
4c_.06	3	0.469	0.075	1.581	0.091	km
4c_.1	3	0.274	0.073	0.959	0.079	km
4c_.35	3	0.089	0.0675	0.319	0.076	km
4c_185	3	0.166	0.068	0.58	0.078	km
4c_70	3	0.446	0.071	1.505	0.083	km
4c_95_SAC_XC	3	0.322	0.074	0.804	0.093	km

The 25 solar systems are randomly installed in different nodes to simulate a residential solar system. The inverter working mode is CONSTANT_PF, system running efficiency is 0.95, single crystal silicon solar panel is to be simulated and the total installed area is 500 ft². The system rated power is 10kW for each solar system.

A load of different nodes is time-varying and ZIP load is to be used in this model. To further simulate the real application, the total load of each resident is the sum of all loads of electrical equipment. The affection to the original network after installing solar generation is shown in Fig.4.As we can see, the total import power from the main substation starts to reduce when solar panel generates the energy to network and the maximum reverse power to grid is around 135kw, which exceeds the reverse power limit of the main substation. The voltage on different buses also increase and close to the upper limit on some buses. For the power losses of this power network, the total power losses with solar system decreases a little bit compared with the original system. In general, the network with solar system minimizes the system power losses but highly affects the voltage stability and network safety.

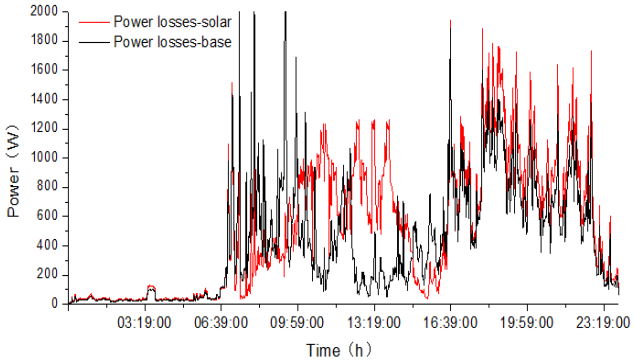

a)Total power losses of distribution network

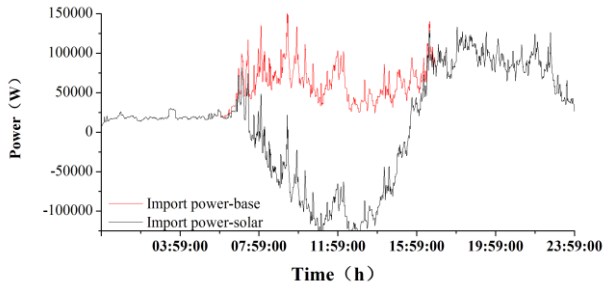

b)Total import power of grid

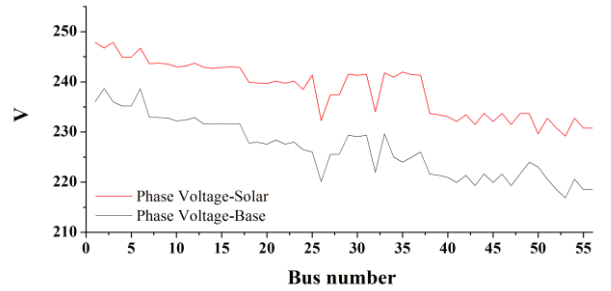

c) Phase voltage of load buses

Fig. 4. The comparison before and after solar PV system is installed

The goal is optimally allocating the distributed energy resources to improve the network stability,while minimizing the total power loss.The function is given

$$F_{cl}=\max \sum_{j=2}^{m} SI_j+\min(P_{loss}) \quad (39)$$

where SI_j is voltage stability index of bus j; P_{loss} is the total active power loss.

Certain constraints should be satisfied to meet the security and real application.the constraints can be divided into two parts:equality constraints and inequality constraints. The inequality constraints are defined as follows:

voltage limit: $U_{\min} \le U_i \le U_{\max}$ (40)

export power limit: $\sum_{i=1}^{N} P_i^{dg} - \sum_{i=1}^{N} P_i^{load} - P_{loss} \le P_{ex\lim it}$ (41)

import power limit: $P^{grid} \le P_{im\lim it}$ (42)

installation power limit of each node: $P_i^{dg} \le P_{ins\lim it}$ (43)

TABLE II. DEFINITION OF INEQUALITY CONSTRAINTS

Name	U_{min}(V)	U_{max}(V)	$P_{exlimit}$(kW)	$P_{imlimit}$(kW)	$P_{inslimit}$(kW)
Value	216	253	400	100	5

The bus numbers of the corresponding installation locations are listed in TableIII,12 battery systems are planned to install and they are distributed in the whole range of distribution network. The optimal results are comprised according to the actual requirements. The further time-schedule optimisation also will be done to further improve the power flow.

TABLE III. OPTIMAL PLACEMENT OF BATTERY SYSTEM

Bus number	34	73	83	208	276	314
Rated power	5	5	5	5	5	5
Bus number	337	347	388	406	489	502
Rated power	5	5	5	5	5	5

From Fig.5, it can be observed that:(1)Compared with the based case without installing battery system, total power losses have been reduced by 10.4%, and voltage stability has been increased by 3.87%;(2)During all periods of one day, the reverse power reduces to 100kW and the maximum import power decreases from 133kW to 117kW. Fig.5 Comparison of distribution network.

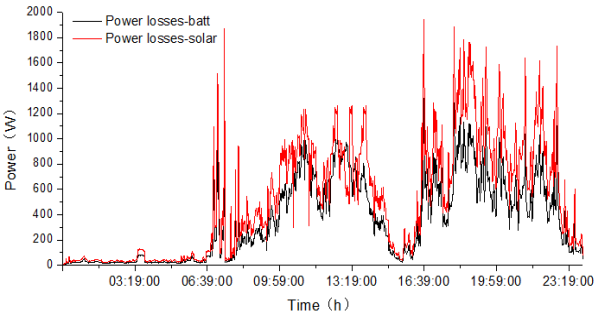

a)Total power losses of distribution network

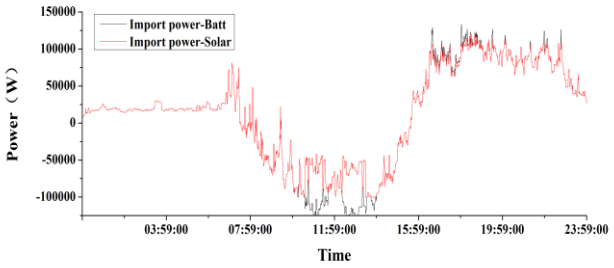

b)Total import power of grid

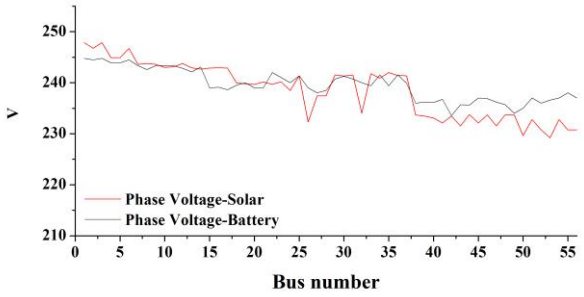

c) Phase voltage of load buses

Fig. 5. The comparison before and after battery system is installed

V. CONCLUSION

Due to high penetration and the intermittent nature of renewable distributed generators, the stability of distributed network faces the high risk. Integrating the storage system is an effective and feasible way to improve the power output performances and compensate for the risk. Conventional planning methodologies are based on pre-designed rated

capacities, however, it is not reasonable in application because of the intermittent nature of renewable generators. Distribution modelling and hybrid optimal algorithms are presented and verified in this paper. As a result, the general conclusion can be drawn:

1) The agent-based distribution network simulation is used and simulates the typical residential network. It Also analyzes the affection to the original network with solar installation.

2) A hybrid optimal algorithm is used to enhance the accuracy of distributed planning. The voltage stability and power losses have an obvious improvement.

In the future, the proposed methodology can be used in the integrated planning of distributed generators. In addition, our next step work will focus on considering the economic factor in hybrid energy storage systems during the optimisation process.

REFERENCES

[1] M. B. Shadmand and R. S. Balog, "Multi-objective optimization and design of photovoltaic-wind hybrid system for community smart DC microgrid," IEEE Trans. Smart Grid, vol. 5, no. 5, pp. 2635–2643, Sep. 2014.

[2] Wang C, Nehrir MH. Analytical approaches for optimal placement of distributed generation sources in power systems. IEEE Trans Power Syst 2004; 19(4): 2068-2076.

[3] M. Farhadi, O. A. Mohammed, "Design and hardware implementation of laboratory-scale hybrid DC power system for educational purpose," in Proc.122nd ASEE Annual Conference and Exposition, Seattle, Washington, USA, 2015.

[4] V. Salehi, A. Mohamed, A. Mazloomzadeh and O.A. Mohammed, "Laboratory-based smart power system, part I: design and system development," IEEE Trans. Smart Grid, vol. 3, no. 3, pp. 1394–1404, 2012.

[5] C. M. Colson and M. H. Nehrir, "Comprehensive real-time microgrid power management and control with distributed agents," IEEE Trans. Smart Grid, vol. 4, no. 1, pp. 617–627, Mar. 2013.

[6] W. Saad, Z. Han, H. V. Poor, and T. Basar, "Game-theoretic methods for the smart grid," IEEE Signal Process. Mag., vol. 29, no. 5, pp. 86–105, Sep. 2012.

[7] L. Noel, J.F. Brodie, W. Kempton, C.L. Archer, C. Budischak, Cost minimization of generation, storage, and new loads, comparing costs with and without externalities, Appl. Energy 189 (March) (2017) 110–121

[8] Sedghi M, Ahmadian A, Aliakbar-Golkar M. Optimal storage planning in active distribution network considering uncertainty of wind power distributed generation. IEEE Trans Power Syst 2016; 31: 304-316.

[9] Santos SF, Fitiwi DZ, Cruz MRM, Cabrita CM, Catalão JP. Impacts of optimal energy storage deployment and network reconfiguration on renewable integration level in distribution systems. Appl Energy 2017; 185: 44-55.

[10] David P. Chassin; Jason C. Fuller; Ned Djilali," GridLAB-D: An agent-based simulation framework for smart grids," Journal of Applied Mathematics,2014.

[11] Da Costa VM, Martins N, Pereira JLR. Developments in the NewtonRaphson power flow formulation based on current injections. IEEE Transactions on Power Systems. 1999.

[12] P. A. N. Garcia, J. L. R. Pereira, S. Carneiro, Jr., V. M. Da Costa, and N. Martins, "Three-phase Power Flow Calculations using the Current Injection Method," IEEE Transactions on Power Systems, vol. 15, no. 2, pp. 508-514, 2000

[13] M.Ahmadi , H. Hosseinzade, H.Sayyaadi; Mohammadi, H.Amir ,H.Kimiaghalam and Farshad. "Application of the multi-objective optimisation method for designing a powered Stirling heat engine: Design with maximized power, thermal efficiency and minimized pressure loss".Renew. Energy 60.pp.313-322, 2013.

[14] IEEE PES Distribution System Analysis Subcommittee's Distribution Test Feeder Working Group,https://ewh.ieee.org/soc/pes/dsacom/